AD 400 285

N-63-3-1

NOLTR 62-159

THEORETICAL CALCULATIONS ON THE SHOCK INITIATION OF LIQUID TNT

NOL

24 AUGUST 1962

UNITED STATES NAVAL ORDNANCE LABORATORY, WHITE OAK, MARYLAND

U. S. NAVAL ORDNANCE LABORATORY

WHITE OAK
SILVER SPRING, MARYLAND

To all holders of NOLTR 62-159 — Change 1
insert change; write on cover 'Change 1 inserted' 1/30/63
Approved by Commander, U.S. NOL — 2 pages

Albert D. Lightbody
By direction

This publication is changed as follows:

Replace page 21 with Change 1 attached

Insert this change sheet between the cover and the title page of your copy.

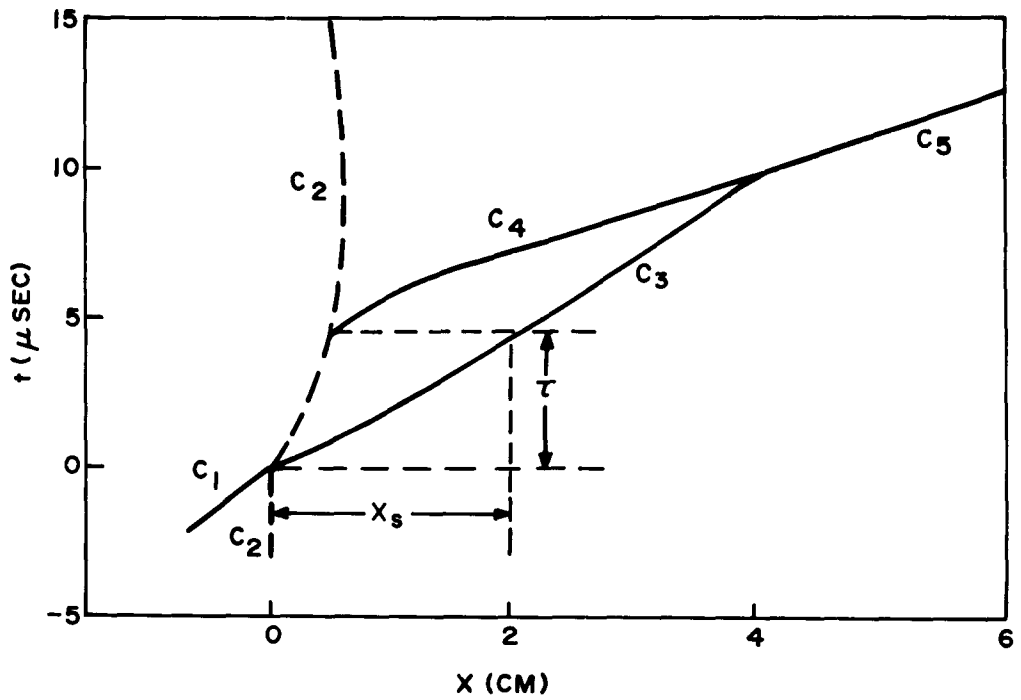

FIG. 4 t, X DIAGRAM SHOWING THE WAVE AND PARTICLE MOTION FOR CASE 2

CHANGE 1

NOLTR 62-159

THEORETICAL CALCULATIONS ON THE SHOCK INITIATION OF LIQUID TNT

By

JULIUS W. ENIG
FRED T. METCALF

ABSTRACT: Theoretical calculations describing the initiation phenomena in homogeneous liquid TNT, produced by shocks between 80 and 89 kilobars, are given. The initiation mechanism and growth to detonation are shown to be in semi-quantitative agreement with experimental results. Upon entering the explosive, the shock wave initiates chemical reaction. After an induction time, the explosive cell that has been heated the longest detonates. The detonation wave, traveling in precompressed explosive with a velocity greater than the steady state velocity in uncompressed explosive, overtakes the decaying initial shock and temporarily overdrives detonation in the uncompressed explosive. The numerical experiments, which are based on finite difference solutions of the partial differential equations of hydrodynamics, show the extreme sensitivity of the induction time to the initiating pressure in idealized one-dimensional gap tests. Of particular interest is the situation at onset of detonation after critical initiation by the attenuated shock from a short donor. In this case, the interface pressure is lower than that in the shock front although the interface temperature is, of course, higher than that of the shock front.

PUBLISHED NOVEMBER 1962

APPROVED BY: Donna Price, Acting Chief
Physical Chemistry Division
CHEMISTRY RESEARCH DEPARTMENT
U. S. NAVAL ORDNANCE LABORATORY
WHITE OAK, SILVER SPRING, MARYLAND

This work was carried out under FR-59, Transition from Deflagration to Detonation. The results represent progress in theoretical treatment of this problem since the model chosen has qualitatively reproduced observed experimental trends.

R. E. ODENING
Captain, USN
Commander

ALBERT LIGHTBODY
By direction

TABLE OF CONTENTS

INTRODUCTION

The initiation of detonation in explosives by shocks has been the subject of a very large number of experimental investigations and a growing number of theoretical calculations. These are well summarized in reviews by Bowden and Yoffee[1], Jacobs[2], Evans and Ablow[3], and Maček[4]. Shock initiation in liquid and solid explosives can be described by physico-chemical interactions that occur in homogeneous and heterogeneous materials, respectively. Therefore, a theoretical description, while difficult, is still simpler for homogeneous liquids than for heterogeneous solids and will be the purpose of this paper. In the following paper[5], theoretical calculations for shock initiation of detonation in heterogeneous solid explosives are given.

Hubbard and Johnson[6] studied the properties of the shock necessary to initiate detonation in homogeneous explosives and found that when an element of explosive was subjected to a shock wave of proper strength a time interval of shock heating existed, called the "induction time", in which very little chemical reaction occurred. Then complete reaction occurred in a relatively short time and a wave of chemical reaction moved forward as a detonation wave. In particular, they gave numerical solutions to the one-dimensional equations representing the conservation of mass, momentum, and energy, the equations of state, and the equation of first-order chemical kinetics for a rectangular pressure pulse applied to the surface of a semi-infinite slab. From these results they drew conclusions as to the relationship between the magnitude of the shock and the duration of the pulse that led to initiation. The method of solution involved the use of the "q" method of von Neumann and Richtmyer[7]. They assumed the same Abel type equation of state to hold for <u>both</u> unreacted explosive and product gas.

Enig[8] obtained numerical solutions of the one-dimensional Navier-Stokes equations, including a first-order chemical reaction term of the Arrhenius type, for the problem of a piston pushing with constant velocity against one surface of a chemically inert slab whose other surface is in intimate contact with a semi-infinite homogeneous explosive. The inert and the explosive were chosen to have the same equation of state. If the shock which is transmitted into the explosive from the inert is sufficiently strong, chemical reaction is initiated at the interface between the inert and the explosive. By choosing the appropriate piston velocity it was possible to produce solutions in which the shock had been transmitted some distance into the explosive before the inert-explosive interface, which had been heated and therefore reacting the longest, detonated. This detonation wave, traveling over shocked explosive, rapidly caught up to the first shock wave and then proceeded as an ordinary detonation wave into the unreacted explosive. Separate equations of state were used for the unreacted explosive and the product gases and, by assuming additive energies and volumes, the equations of state of the intermediate products in the reaction zone were obtained. By stopping the piston after a finite time it was shown that, for the constants used, if as little as one or two percent of an element of explosive had reacted, a detonation wave would subsequently be established, would propagate, and could not be quenched by any reasonably strong rarefaction-wave which might appear on the scene. As Hubbard and Johnson also found for very temperature sensitive reactions, the time necessary for the major portion of an element of explosive to react was small compared to the hydrodynamic time necessary to influence motion. However, these conclusions were not always true for the more sophisticated numerical experiments to be described here.

In this paper numerical experiments are described which show that the initiation of detonation in homogeneous liquid TNT is a result of shock heating and that the initiation process is basically one of thermal explosion. These one-dimensional calculations have been made more realistic by impressing upon the liquid TNT acceptor a pressure pulse which is the result of a Taylor wave[9] from an explosive donor, the shock from which passes through an inert attenuator before reaching the attenuator-TNT interface. The set-up is shown in Fig. 1 where X = 0 is the point at which the donor explosive is initiated. In these calculations, both the lengths of donor explosive, d_{donor}, and of the gap material, d_G, have been varied in such a way as to show the coupled effects of the amplitude of the transmitted shock pressure and the slope of the pressure-distance curve behind this shock in the liquid TNT. Previous theoretical calculations[6,8] assumed that the state behind the shock front was uniform. For fixed d_{donor}, a critical gap length, d_G^*, has been determined such that if this length is slightly exceeded detonation will not occur in the liquid TNT. These calculations may be considered as one-dimensional idealized versions of the experimental "gap tests"[5]; the critical gap length and resulting transmitted shock amplitude in the TNT is then equivalent to the "50% gap length and pressure" values. The numerical experiments show that the reaction rate first becomes important at the attenuator-liquid TNT interface, where the temperature has been highest for the longest time, and that detonation first occurs here even though the transmitted shock may already have penetrated the TNT to a depth of several centimeters. The most recent, very precise physical experiments[10] on homogeneous explosives support this conclusion.

Section II contains the appropriate hydrodynamic equations to be solved. The equations of state for the unreacted explosive, product gases, reactive mixture, and gap material are given

in Sec. III. The finite difference scheme for solving the partial differential equations of hydrodynamics is described in Sec. IV. Section V gives the results of the one-dimensional gap test calculations made for liquid TNT. Finally, these theoretical results are compared to actual experimental results in Sec. VI.

II. HYDRODYNAMIC EQUATIONS

The unsteady one-dimensional hydrodynamic equations are most conveniently given in the Lagrangean form since this reveals where each particle of fluid came from initially and hence, supplies more information than the Eulerian form. Importantly, shocks and moving contact discontinuities can be more easily followed, and mass is automatically conserved. Let the Lagrangean coordinate x denote the Eulerian space coordinate X of a small fluid element at time t = 0, and X = X(x,t) denote the position of that same fluid element at time t > o, where x and t are the independent variables. The equations representing the conservation of mass, momentum, and energy for a single viscous fluid are respectively,

$$\partial V/\partial t = V^{o}(x)\partial u/\partial x, \tag{1}$$

$$\partial u/\partial t = V^{o}(x)\partial(G-P)/\partial x \tag{2}$$

$$\partial E/\partial t = V^{o}(x)(G-P)\partial u/\partial x \tag{3}$$

where

$$G = \tfrac{4}{3}\mu[V^{o}(x)/V]\ \partial u/\partial x,^{11} \tag{4}$$

and E, P, V, **u**, and μ are respectively, the specific internal energy, pressure, specific volume, particle velocity, and coefficient of viscosity. The superscript o will always refer to initial conditions. The equation of state,

$$E = r(P,V), \tag{5}$$

then completes the hydrodynamic description, provided the fluid species are unchanged. However, in the explosive an irreversible first-order chemical reaction,

$$[\ell] \rightarrow [g], \tag{6}$$

is postulated, where the chemical kinetic equation which governs the conversion of unreacted liquid explosive $[\ell]$ to product gas $[g]$ is

$$\partial w/\partial t = -Z\ w \exp\left[-E^{\ddagger}/(RT)\right]. \tag{7}$$

Here, w, T, Z, $E^{\ddagger}$, and R are respectively, the mass fraction of unreacted explosive, temperature, frequency factor, activation energy, and gas constant. To determine the temperature the additional equation of state,

$$E = s(T,V), \tag{8}$$

must be given. Equations (1), (2), (3), (4), (5), (7), and (8) are seven equations defining the seven dependent variables E, P, V, T, u, G, and w in terms of x and t. Finally, the Eulerian position X(x,t) of the particle initially at x can be found from

$$\partial X/\partial t = u. \tag{9}$$

It should be noted that E and V are the specific energy and volume of an element of mass which may be a mixture of liquid and gas. The element is assumed to be a uniform mixture with uniform pressure and temperature.

III. EQUATIONS OF STATE

For chemical reactions that involve a finite reaction zone, it is necessary to describe not only the initial and final chemical states but also the intermediate ones. This can be done in a simple manner if it is assumed that E and V (of the intermediate mixture) are equal to the sum of the internal energies and volumes of liquid explosive and gaseous product, i.e.,

$$V = wV_\ell + (1-w)V_g, \tag{10}$$

$$E = wE_\ell + (1-w)E_g, \tag{11}$$

where the subscripts ℓ and g refer to the liquid TNT and product gas respectively, and V_ℓ, E_ℓ, V_g, and E_g are respectively, the specific volume and energy that the pure liquid and gas would have if each existed in isolation at the pressure and temperature that the mixture is assumed to have.

Since the equation of state is so important in determining the fluid flow and chemical reaction characteristics, it is desirable to introduce separate equations of state for the liquid TNT and product gases rather than use a single equation of state for both reactant and product. For the product gas, the equations of state used are

$$E_g = PV_g/(\gamma_g - 1), \tag{12}$$

$$E_g = c_{v,g}T. \tag{13}$$

For the liquid TNT, the E,P,V equation of state is taken as

$$E_\ell = E_\ell^o + \left[(P+B)V_\ell - (P^o+B)V_\ell^o\right] /(\gamma_\ell - 1), \tag{14}$$

where

$$B = \rho_\ell^o (c_\ell^o)^2 \tag{15}$$

is determined from the thermodynamic identity defining the adiabatic sound speed c,

$$c^2 = V^2 \left[P(\partial P/\partial E)_V - (\partial P/\partial V)_E \right], \tag{16}$$

and the initial energy, E_ℓ^o, is as yet undetermined. The quantities c_ℓ^o and γ_ℓ are evaluated from experimental data in the following manner. From the three Rankine-Hugoniot shock equations,

$$P_H = \rho_\ell^o \, u_H U, \tag{17}$$

$$E_H - E_o = \tfrac{1}{2} P_H (V_\ell^o - V_H), \tag{18}$$

$$u_H^2 = P_H (V_\ell^o - V_H), \tag{19}$$

and Eq. (14), it can be easily found that

$$(2U/u_H) - 1 = 2(c_\ell^o)^2/(U u_H) + \gamma_\ell, \tag{20}$$

where the subscript H refers to values for the shocked state, U is the shock velocity in liquid TNT, and P^o = 1 bar has been neglected. Use of the experimental U, u_H data of Garn[12] for liquid TNT to 111 kilobars, and a least-squares straight line fit for $(2U/u_H)-1$ *vs.* $2/(Uu_H)$ in Eq. (20), gives for the square root of the slope and the intercept respectively, c_ℓ^o = 0.2469 cm/μsec and γ_ℓ = 3.178. With these constants, the value of U computed from Eq. (20) for any experimental value of u_H differs from the experimental value of U by at most 3.6%. Since Garn's experimental data had a typical spread of ±2.5% in shock velocity, it is felt that Eq. (14) represents the Hugoniot data sufficiently accurately for the computations to be described.

Furthermore, along an isentrope through P^o, V_ℓ^o, Eq.(14) reduces to

$$P = B\left[(V_\ell^o/V_\ell)^{\gamma_\ell} - 1\right]/\gamma_\ell \quad , \tag{21}$$

which is the adiabatic Tait equation[13] used to describe water to pressures of 80 kilobars. Equation (14) and the assumption that the specific heat at constant volume $c_{v,\ell}$ is a constant defines the E,V,T equation of state,

$$E = E_\ell^o + c_{v,\ell}T + \left[AV_\ell^{1-\gamma_\ell} + (\gamma_\ell - 1)EV_\ell/\gamma_\ell - (P^o + B)V_\ell^o\right]/(\gamma_\ell - 1), \tag{22}$$

where

$$A = (V_\ell^o)^{\gamma_\ell}\left[P^o + B/\gamma_\ell - (\gamma_\ell - 1)c_{v,\ell}T^o/V_\ell^o\right] . \tag{23}$$

That this is true can be readily verified by noting that Eqs. (14) and (22) satisfy the thermodynamic identity,

$$(\partial E/\partial V)_T = T(\partial P/\partial E)_V(\partial E/\partial T)_V - P. \tag{24}$$

Along an isentrope,

$$T = KV^{1-\gamma_\ell}, \tag{25}$$

where K is a constant that depends on the particular isentrope. Let Q be the internal energy difference between reactant and product at the initial pressure and temperature, i.e.,

$$Q = E_\ell(P^o, T^o) - E_g(P^o, T^o). \tag{26}$$

Substitution of Eqs. (13) and (22) into (26) then defines E_ℓ^o as

$$E_\ell^o = Q + c_{v,g}T^o \ . \tag{27}$$

The inert gap material is assumed to have a P,V Hugoniot curve given by[14]

$$P = 58.4(0.847 - V_G)/(0.272 + V_G)^2 , \qquad (28)$$

where P and V_G are in kilobars and cm^3/g, respectively; the isentropic expansion curve is assumed to follow the Hugoniot. It was shown by Walsh and Christian[15] that the use of the P,V Hugoniot to represent the isentropic expansion curve for any material is equivalent to minimizing $u_{fs} - u_H$, where

$$u_{fs} - u_H = \int_0^{P_H} (\rho c)^{-1} dP, \qquad (29)$$

u_{fs} is the free surface velocity at P = 0, and $u_{fs} - u_H$ is the increment in particle velocity due to a centered single rarefaction wave from the shocked state P_H, u_H to $0, u_{fs}$.

The following constants are used for each fluid:

Tetryl(donor explosive)[16]: P^o = 1 bar, ρ^o = 1.63 g/cm^3, T^o = 300°K, Q = 1047 cal/g

Tetryl product gas[16]: γ_g = 2.69

Liquid TNT(acceptor explosive): P^o = 1 bar, V_ℓ^o = 0.679 cm^3/g[12], T_ℓ^o = 354°K[12]

Q = 836 cal/g, γ_ℓ = 3.178, c_ℓ^o = 0.2469 cm/μsec

$c_{v,\ell}$ = 0.328 cal/(g deg)[17], B = 89.805 kbar, A = 1.6998 kbar $(cm^3/g)^{3.178}$

E‡ = 34.4 kcal/mole[18], Z = $10^{11.4}$ sec^{-1} [18]

The values of Q = 836 cal/g and γ_g = 2.689 for the detonation of liquid TNT were computed by solving for Q and γ_g from the equations,

$$(\gamma_g+1)P_{CJ} = \rho_\ell^o D^2$$
$$2(\gamma_g^2-1)Q = D^2$$

which are valid for a Chapman-Jouget detonation, where the detonation velocity, D = 0.66 cm/μsec, was measured by L. B. Seely, Jr.[19], and P_{CJ} = 171.8 kbars was determined by Garn[20]. The initial temperature and density in their work were respectively, T^o = 365°K and ρ_i^o = 1.455 g/cm^3.

IV. FINITE DIFFERENCE EQUATIONS

In order to carry out the numerical solution of Eqs. (1) - (5), and (7) - (9), they are replaced by an equivalent system of finite difference equations. The exact form of these equations is governed by stability considerations and a stability analysis as proposed by von Neumann[7] has been carried out in order to verify that small errors will not grow during the computations. The difference equations used for the numerical calculations are as follows:

$$u_{j+\frac{1}{2}}^{n+\frac{1}{2}} - u_{j+\frac{1}{2}}^{n-\frac{1}{2}} = (\Delta t^n/\Delta x)V_{j+\frac{1}{2}}^o(G_{j+1}^n - G_j^n - P_{j+1}^n + P_j^n), \tag{30}$$

$$V_j^{n+1} - V_j^n = (\Delta t^{n+\frac{1}{2}}/\Delta x)\, V_j^o(u_{j+\frac{1}{2}}^{n+\frac{1}{2}} - u_{j-\frac{1}{2}}^{n+\frac{1}{2}}) , \tag{31}$$

$$E_j^{n+1} - E_j^n = \tfrac{1}{2}(\Delta t^{n+\frac{1}{2}}/\Delta x)V_j^o(G_j^{n+1} + G_j^n - P_j^{n+1} - P_j^n)(u_{j+\frac{1}{2}}^{n+\frac{1}{2}} - u_{j-\frac{1}{2}}^{n+\frac{1}{2}}) , \tag{32}$$

$$G_j^{n+1} = \frac{8}{3}\mu\, V_j^o(u_{j+\frac{1}{2}}^{n+\frac{1}{2}} - u_{j-\frac{1}{2}}^{n+\frac{1}{2}})/(V_j^{n+1} + V_j^n) , \tag{33}$$

$$E_j^{n+1} = r(P_j^{n+1}, V_j^{n+1}) , \tag{34}$$

$$w_j^{n+\frac{1}{2}} - w_j^{n-\frac{1}{2}} = -\tfrac{1}{2}Z\Delta t^n(w_j^{n+\frac{1}{2}} + w_j^{n-\frac{1}{2}})\exp\left[-E^*/(RT_j^n)\right] , \tag{35}$$

$$E_j^{n+1} = s(T_j^{n+1}, V_j^{n+1}) , \tag{36}$$

$$X^{n+\frac{1}{2}}_{j+\frac{1}{2}} - X^{n-\frac{1}{2}}_{j+\frac{1}{2}} = \tfrac{1}{2}\Delta t^{n}(u^{n+\frac{1}{2}}_{j+\frac{1}{2}} + u^{n-\frac{1}{2}}_{j+\frac{1}{2}}) \ , \tag{37}$$

$$X^{n+1}_{j} - X^{n}_{j} = \tfrac{1}{2}\Delta t^{n+\frac{1}{2}}(u^{n+\frac{1}{2}}_{j+\frac{1}{2}} + u^{n+\frac{1}{2}}_{j-\frac{1}{2}}) \ , \tag{38}$$

$$\Delta t^{n} = \tfrac{1}{2}(\Delta t^{n+\frac{1}{2}}+\Delta t^{n-\frac{1}{2}}) \ , \qquad V^{o}_{j+\frac{1}{2}} = \tfrac{1}{2}(V^{o}_{j+1} + V^{o}_{j}), \tag{39}$$

where

$$j = 0,1,2,\ldots, J; \ n = 0,1,2,\ldots$$

$$u^{n+\frac{1}{2}}_{j+\frac{1}{2}} = u(x+\tfrac{1}{2}\Delta x, t+\tfrac{1}{2}\Delta t), \ w^{n-\frac{1}{2}}_{j} = w(x+\Delta x, t-\tfrac{1}{2}\Delta t), \text{ etc.}$$

Here x is defined as shown in Fig. 1 and Δx (which, with more precision but also more notational complication, should be written as Δx_i) is the mesh size in the ith fluid, where i = 1, 2, 3 refers to respectively, the donor explosive, inert gap, and acceptor explosive (liquid TNT). The total number of mesh points used in the computations was 130, i.e., J = 129.

If all the variables are known at $t^{n-\frac{1}{2}}$ and t^{n}, the times corresponding to the nth time step ($t^{-\frac{1}{2}}<0, t^{o} = 0$), and the outer boundary conditions are prescribed at j = 0 and j = J, then the values at the new times, $t^{n+\frac{1}{2}} = t^{n-\frac{1}{2}}+\Delta t^{n}$ and $t^{n+1} = t^{n}+\Delta t^{n+\frac{1}{2}}$ are computed as follows. Let $X^{n}_{j+\frac{1}{2}}$, $j = I_1, I_2$, $0<I_1<I_2<J$, be the instantaneous positions of the donor explosive-inert and inert-acceptor explosive interfaces (contact discontinuities) respectively. Therefore $u^{n}_{j+\frac{1}{2}}$, $j = I_1, I_2$, are the velocities of these interfaces. These velocities must be computed from the special formula,

$$u^{n+\frac{1}{2}}_{I+\frac{1}{2}} = u^{n-\frac{1}{2}}_{I+\frac{1}{2}} + (\Delta t^{n}/\Delta x)\,\zeta^{n}_{I+\frac{1}{2}}, \ I = I_1 \text{ or } I_2 \tag{40}$$

where

$$\zeta = V^{o}(x)\partial(G-P)/\partial x \ . \tag{41}$$

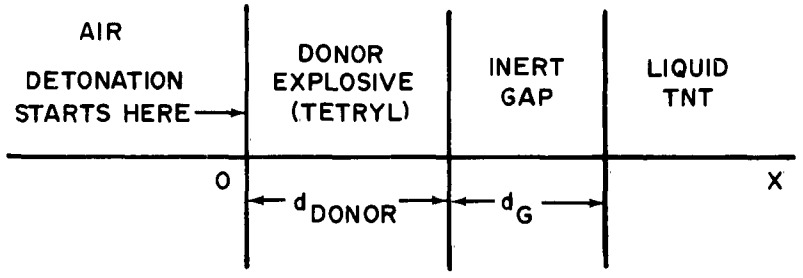

FIG. 1 IDEALIZED ONE-DIMENSIONAL GAP TEST

The unknown $\left\{{}^{n}_{I+\frac{1}{2}}\right.$ is obtained by expanding $\left\{{}^{n}_{I+\frac{1}{2}}\right.$ to first order about the points at $I-\frac{1}{2}$, I, I+1, $I+\frac{3}{2}$ and solving the resulting four equations in the four unknowns, $\left\{{}^{n}_{I+\frac{1}{2}}\right.$, $(G-P)^{n}_{I-\frac{1}{2}}$, $(G-P)^{n}_{I+\frac{1}{2}}$, and $(G-P)^{n}_{I+\frac{3}{2}}$, for $\left\{{}^{n}_{I+\frac{1}{2}}\right.$. From Eq.(30), $u^{n+\frac{1}{2}}_{j+\frac{1}{2}}$, $0\le j\le J-1$, $j\neq I_1, I_2$, are then computed. Equations (35),(31), and (33) then give $w^{n+\frac{1}{2}}_{j}$, V^{n+1}_{j}, and G^{n+1}_{j}, $I\le j\le J-1$.

The time step $\Delta t^{n+\frac{1}{2}}$ is calculated from

$$\Delta t^{n+\frac{1}{2}} = \min_{0\le j\le J}\left\{(\Delta t^{n+\frac{1}{2}}_{j})_{\text{hydro.}}, (\Delta t^{n}_{j})_{\text{chem.}}\right\}. \qquad (42)$$

At every point (including those in the reaction zone where $0<w^{n-\frac{1}{2}}_{j}<1$) the hydrodynamic time step $(\Delta t^{n+\frac{1}{2}}_{j})_{\text{hydro.}}$ is determined from the stability criterion,

$$\frac{16\mu}{3}\frac{(V^{o}_{j})^{2}}{V^{n}_{j}+V^{n-1}_{j}}\frac{\Delta t^{n+\frac{1}{2}}_{j}}{(\Delta x)^{2}} + \left\{\left(\frac{V^{o}_{j}c^{n}_{j}}{V^{n}_{j}}\right)^{2} - \tfrac{1}{2}(V^{o}_{j})^{2}(G^{n}_{j}+G^{n-1}_{j})\left[\left(\frac{\partial P}{\partial E}\right)_{V}\right]^{n}_{j}\right\}\left(\frac{\Delta t^{n+\frac{1}{2}}_{j}}{\Delta x}\right)^{2} \le 1. \qquad (43)$$

However, in the reaction zone, c^{n}_{j} and $\left[(\partial P/\partial E)_{V}\right]^{n}_{j}$ are computed by assuming that w = 1. This is much simpler than taking into account the change in w and has worked very well without any loss in computational time. In the reaction zone the critical chemical time step is

$$(\Delta t^{n}_{j})_{\text{chem.}} = (2/Z)\exp\left[E^{*}/(RT^{n}_{j})\right], \qquad (44)$$

which is derived from Eq. (35) by letting $w^{n+1}_{j} = 0$.

For unreacted liquid TNT and product gas, Eq. (34) is defined by Eqs. (12) and (14) in which E^{n+1}_{j} is linear in P^{n+1}_{j}. Hence, Eqs. (32) and (34) can be solved explicitly for E^{n+1}_{j} and P^{n+1}_{j}.

The temperature T_j^{n+1} then follows from Eq. (36) (See Eqs. (13) and (22)). For the gap material P_j^{n+1} is computed from Eq. (28), and E_j^{n+1} follows from Eq. (32). However, for the reactive mixture the procedure is much more complex. Equations (10), (11), (12), (13), (14), and (22) evaluated at j, n+1 and Eq. (32) are seven equations in the nine variables E_j^{n+1}, P_j^{n+1}, T_j^{n+1}, $V_{\ell,j}^{n+1}$, $V_{g,j}^{n+1}$, $E_{\ell,j}^{n+1}$, $E_{g,j}^{n+1}$, V_j^{n+1}, and $w_j^{n+\frac{1}{2}}$. But V_j^{n+1} and $w_j^{n+\frac{1}{2}}$ are already known so that the first seven variables listed can be determined. However, this first involves the extraction of the root $V_{\ell,j}^{n+1}$ of the equation

$$\Phi(\lambda) \equiv (b_1+b_2\lambda+b_3\lambda^2)\lambda^{\gamma} + (b_4+b_5\lambda)\lambda = 0, \qquad (45)$$

which is carried out to five place accuracy. Here, b_1, b_2, b_3, b_4, and b_5 are functions of the flow variables which are already known at n or n+1.

During the progress of every machine computation, the conservation of mass, momentum, and energy were continually checked. Mass and momentum were extremely well conserved; energy losses were at most 1 or 2%.

V. ONE-DIMENSIONAL GAP TEST CALCULATIONS

The one-dimensional idealized version of the gap test is shown in Fig. 1. A number of numerical experiments were performed on an IBM 7090 computer in which the length of the donor explosive (Tetryl), d_{donor}, was fixed and the length of the gap d_G was varied until detonation in the liquid TNT was just barely possible. For gaps larger than this critical length d_G^*, detonation never propagated; for smaller gaps detonation always propagated. The results of these machine computations are given in Table 1. Here P_t is the value of the pressure of the transmitted shock as it enters the liquid

TNT. For Cases 1 - 5, the shock initiated reaction upon entering the liquid TNT and had advanced a distance x_s into the explosive at the time the explosive cell at the gap-explosive interface detonated. For Cases 2, 3, and 4, the shock amplitude continuously decreased for $t<\tau$. The induction time τ is the "cooking" time of that cell after the shock passed over it.

The pressure distribution at various times is shown in Fig. 2 for Case 2. In Fig. 2(a) the Taylor detonation wave has already reflected off the product gas-attenuator interface and a reflected rarefaction wave is moving back into the product gas while a shock is transmitted into the gap material. Only the rightmost part of the product gas is shown since most of the gas is expanding to the left into a vacuum (approximating air at several bars). In Fig. 2(b) the progress of the shock in the gap is shown; and in Fig. 2(c) the shock has reflected off the gap-liquid TNT interface with the result that higher amplitude shocks are moving into the gap and into the explosive. In Fig. 2(d) the almost discontinuous rise in pressure at the interface, due to reaction, can be seen. Now, in a very short time complete reaction occurs as shown in Fig. 2(e). The detonation wave, traveling faster than the forward shock front, rapidly catches up to the latter (Figs. 2(f) and 2(g)), and then proceeds as an ordinary detonation wave (Fig. 2(h)). In Figs. 2(d) to 2(g), it can be seen that the amplitude of the transmitted shock is decreasing because of rarefaction waves from the rear. Though the pressure at the gap-liquid TNT interface is lower than at the shock front the temperature is always higher because of the release of energy in the conversion of explosive to product gas. In Fig. 3 the pressures at the interface and at the shock front are plotted as functions of time for Case 2, where the time scale has been shifted such that the new origin coincides with that (real) time at which

Fig. 2 The pressure distribution in the one-dimensional gap test for various values of t for Case 2. The heavy vertical lines A, B, C, and D represent respectively, the air-product gas interface, the product gas-attenuator interface, the attenuator-liquid TNT (or liquid TNT product gas) interface, and the liquid TNT-air interface. Each dot represents a mass point whose initial position is given by the Lagrangean coordinate x. The motion of any mass point in the X direction can be followed by observing the motion of that same dot (provided the observer has a pair of telescopic eyes). The values of t (μsec), as measured from the instant at which the shock first entered the explosive, are as follows: (a) -7.93, (b) -2.80, (c) 0.45, (d) 3.84, (e) 4.67, (f) 6.15, (g) 7.85, (h) 10.74.

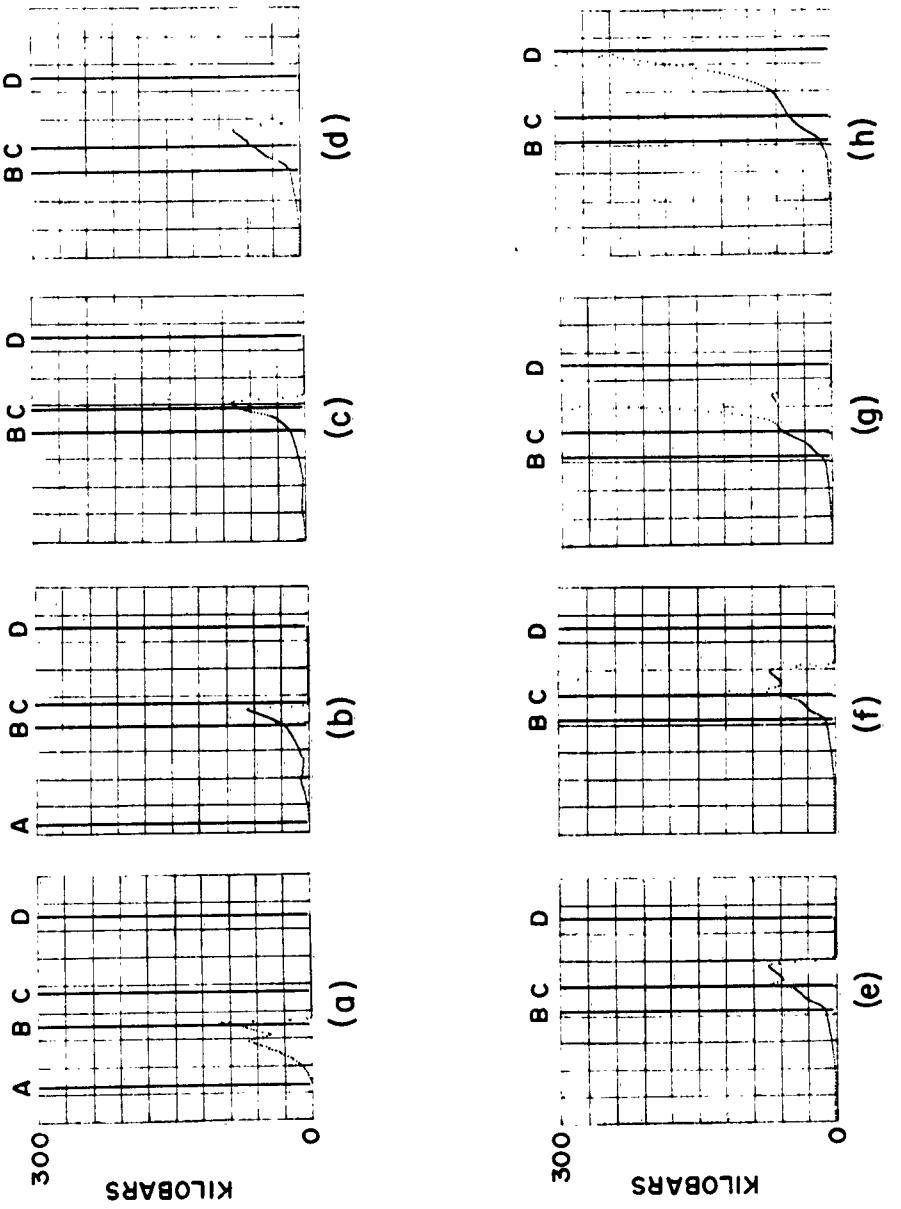

FIG. 2 THE PRESSURE DISTRIBUTION IN THE I-D GAP TEST FOR VARIOUS VALUES OF t FOR CASE 2

the shock first entered the explosive. Complete reaction occurs at $\tau = 4.32$ μsec. In Case 2 the rarefaction wave attenuates the shock that has progressed into the liquid TNT interior, and chemical reaction at this front is never able to compete successfully with the rarefaction wave. This wave effectively annihilates any compression waves which may originate at the slowly reacting interface and which would tend to move in the direction of, and thus reinforce, the shock front.

For Cases 1 and 5, the results are similar to Case 2, except that at the gap-liquid TNT interface the pressure (and temperature) continuously increases with time during reaction as shown in Fig. 3 for Case 5. Therefore, the pressure and temperature decrease monotonically in the direction of the shock front. In these cases it is not possible to decide whether the pressure at the shock front decreases or increases with time for $t < \tau$ since the numerical method does not define a sharp shock front and, hence, it is not possible to evaluate accurately the pressure.

It is at the interface that the interaction between the shock pressure amplitude and the varying pressure distribution behind the shock is seen. In previous work, the state behind the initial shock was uniform, thus leading to an increase in both P and T at the piston-explosive interface[6] or at the inert gap-explosive interface[8]. However, in Case 2, the pressure at the interface decreases with time during most of the "cooking" period because of the rarefaction wave from the rear. Increasing the transmitted shock pressure and the pressure gradient at the interface, as in Case 1, now leads to a monotonic pressure increase with time at the interface. Thus, here the effect of pressure amplitude is more important in increasing the reaction rate (through higher temperatures) than that of increased pressure gradient in decreasing the reaction rate (through

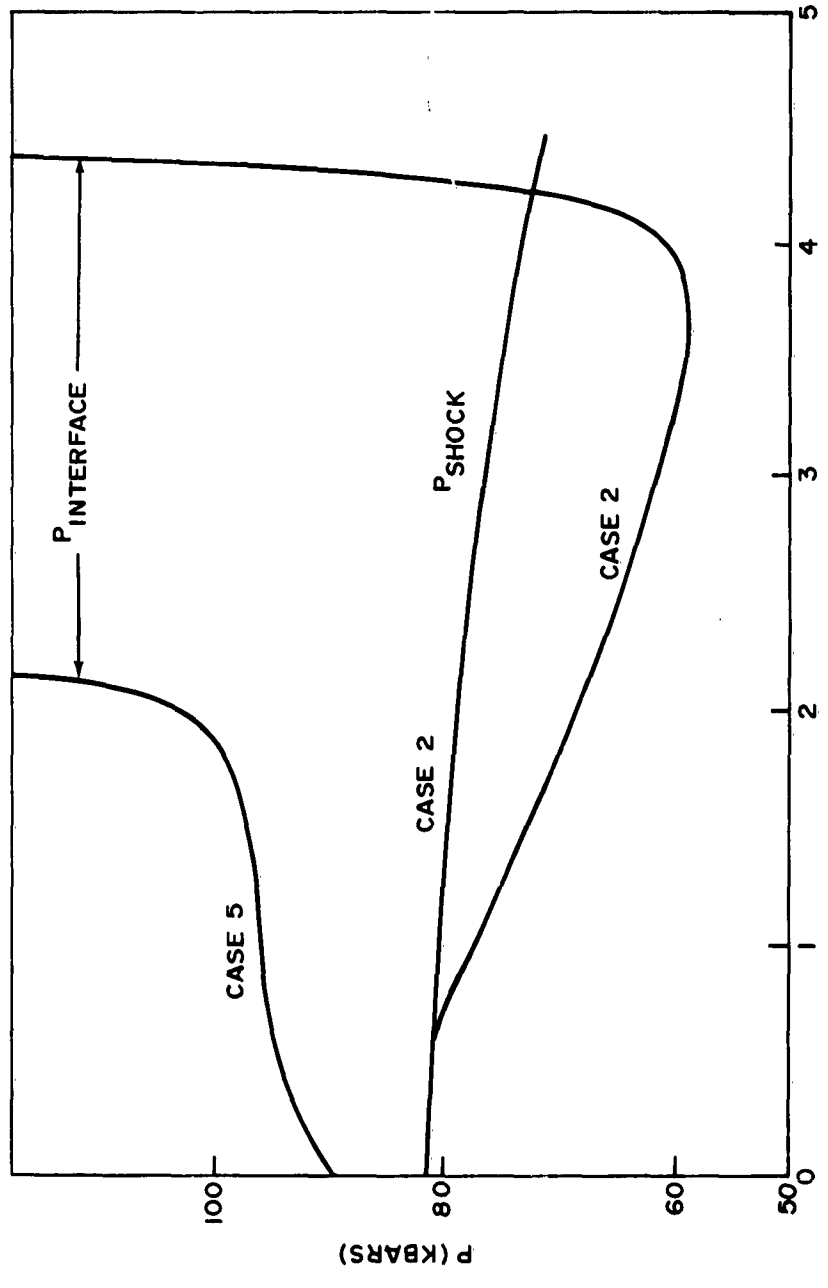

FIG. 3 PRESSURES AT THE ATTENUATOR-LIQUID TNT INTERFACE AND AT THE SHOCK FRONT FOR CASES 2 AND 5

lowering the temperature).

The t,X diagram is particularly informative for showing the wave and particle motion and this is depicted in Fig. 4 for Case 1. Only motion in the vicinity of the gap-liquid TNT interface is shown. Curve C_1 represents the motion of the shock wave in the gap before it strikes the gap-explosive interface. C_2 represents the path of the interface which moves to the right with the local particle velocity while a transmitted shock wave with decreasing velocity moves along C_3 into the explosive. Actually, for the first part of its travel along C_3, the shock front immediately initiates chemical reaction. High-order detonation originates at the interface after a time τ and proceeds through the pre-shocked and very slightly reacted material (0 to 5 percent reacted) along C_4 until the detonation overtakes the transmitted shock at the transition point A and passes into the unshocked explosive along C_5. A similar description holds for Cases 1 and 5 (except perhaps for the shock velocity in the liquid TNT before detonation).

Interesting results were obtained in Case 3 with $d_G = 2.93$ cm and with $d_{donor} = 2.54$ cm (i.e., a perturbation of Case 2). As in Case 2, the first explosive cell detonated, but subsequently the detonation was quenched by the rarefaction wave from the rear and no more than that one cell ever reacted to completion. This sequence of events is shown in Fig. 5. A slight change to $d_G = 2.94$ cm (i.e., Case 4) resulted in failure to detonate at any point. In other words, $d_G^* = 2.92$ cm can be very accurately determined.

VI. COMPARISON OF THEORETICAL WITH EXPERIMENTAL RESULTS

Extensive experiments on the shock initiation of detonation in homogeneous explosives were performed by Campbell, Davis, and Travis[10]. Most of the work was done on nitromethane, but liquid

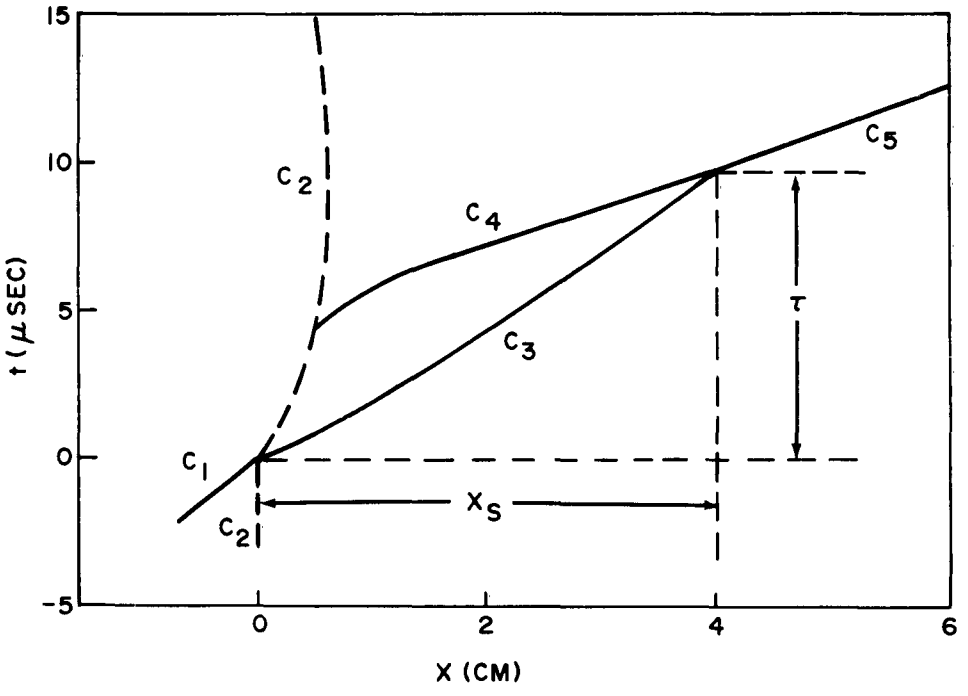

FIG. 4 t, X DIAGRAM SHOWING THE WAVE AND PARTICLE MOTION FOR CASE 2

Fig. 5 The pressure distribution in the one-dimensional gap test for various values of t for Case 3. Reaction begins at the attenuator-liquid TNT interface in (a); complete reaction at interface in (b); quenching of the reaction by rarefaction wave in (c) and (d). See Fig. 2 for definition of the lines A, B, C, and D. The values of t (μsec), as measured from the instant at which the shock first entered the explosive, are as follows: (a) 4.45, (b) 5.40, (c) 6.36, (d) 10.95.

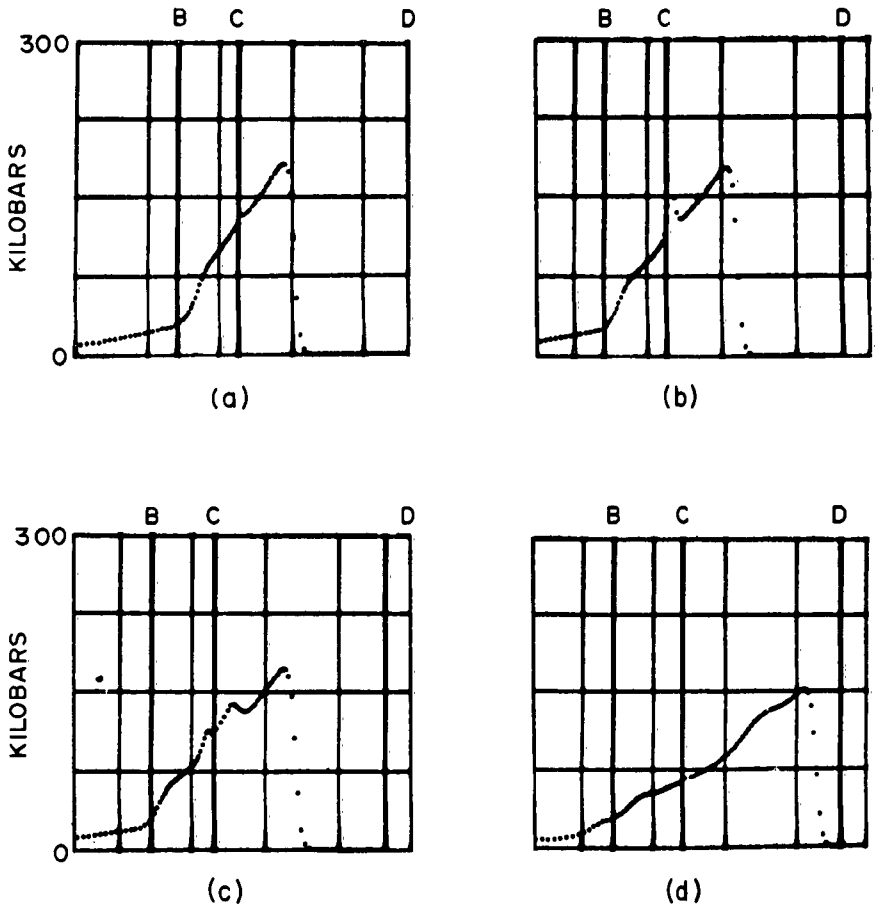

FIG. 5 THE PRESSURE DISTRIBUTION IN THE 1-D GAP TEST FOR VARIOUS VALUES OF t FOR CASE 3

TNT, liquid DINA, Dithekete 13, and single crystals of PETN were shown to behave in the same way. Plane wave lenses were combined with additional high explosive and an inert shock-attenuator to produce a shock wave of desired amplitude in the acceptor explosive. The resulting t,X representation of the initiation behavior of the homogeneous explosives is qualitatively similar to that shown in Fig. 4[21]. Their experimental results show that the initial shock wave in a homogeneous explosive has a constant or slightly decaying velocity as a function of time; the computations for Case 2 show a slightly decaying shock velocity as evidenced by the curvature of C_3 in Fig. 4 or by the decreasing shock pressure in Fig. 3. The experimental results show that small changes in the initial transmitted shock pressure P_t lead to large changes in the induction time τ; the theoretical computations listed in Table I show the same characteristic. The experimental work indicates that the detonation wave overtakes the transmitted shock and temporarily overdrives detonation in the unshocked explosive ahead of it. For nitromethane the detonation velocity increase is approximately 10% and the velocity decreases in a few microseconds to normal detonation velocity; the calculations show a slight overshoot along C_5 in Fig. 4 that disappears after about 1 μsec. The preliminary initiation data[10] for liquid TNT, initially at 358°K, gave as the initiating pressure, 125 kilobars, and as the induction time, 0.7 μsec. This compares with a pressure of 81 - 89 kilobars and induction times of several μsecs from Table I. The discrepancy in the initiating pressures between the experimental and theoretical results may be due to the equation of state, Eq. (14), which represents the experimental U, u_H Hugoniot relatively faithfully, but which can lead to large errors in the temperature (and through the chemical kinetics, to large errors in the initiating pressure) if c_v is not really a constant as assumed in the

TABLE I. Summary of calculational results for liquid TNT. x_s is the distance from the initial position of the gap-liquid TNT interface to the shock front position when complete reaction first occurred at the interface (see Fig. 4). τ is the time interval between the time that the shock first entered the liquid TNT and the time complete reaction first occurred at the gap-liquid TNT interface (see Fig. 4).

Case	d_{donor} cm	d_G cm	P_t kbar	x_s cm	τ μsec
1	2.54	2.70	85	0.7	1.5 [e]
2	2.54	2.92 [a]	81	1.9	4.3
3	2.54	2.93 [b]	80<P<81	2.6	6.4
4	2.54	2.94 [c]	80<P<81	∞	∞
5	15.24	15.1 [d]	89	1.5	2.2 [e]

[a] $d_G = d_G^*$

[b] The first liquid TNT mass cell went to complete reaction but the detonation was subsequently quenched by the rarefaction wave and no other explosive cells went to complete reaction.

[c] 19% of the first liquid TNT mass cell reacted. The rarefaction wave subsequently quenched all further reaction and detonation was never initiated in Case 4.

[d] $d_G < d_G^*$ for this Case.

[e] Why is τ greater for Case 5 than for Case 1 since P_t is greater and the pressure gradient is smaller at the gap-liquid TNT interface? This is probably due to the difference in the

TABLE I (Continued)

viscosities μ of the gap material between Cases 1 - 4 (the same) and Case 5. While the numerical scheme spreads the major part of the shock front over 5 or 6 cells, there always exists a low pressure perturbation that moves ahead of the main shock front and hence slightly changes the initial conditions that the shock front sees. These perturbations are of slightly different magnitude for Cases 1 and 5. The result is that the shock temperature does not converge as quickly to its true value (an upper bound for the numerical temperature) for Case 5 as it does for Case 1. This fact explains the inversion of the values of τ, which is a very sensitive function of temperature.

It should be mentioned that the precursor shock, caused by use of an artificial viscosity, is minimized by testing the relative change in the volume at each time step and by bypassing the hydrodynamic calculations if this relative volume change is less than 10^{-6}.

derivation of Eq. (22)[22]. Also, errors in the evaluation of $E^{\ddagger}$ and Z, or changes in these values with increased P and T, can easily force the initiating temperature and (through the equation of state) the initiating pressure P_t upwards. Furthermore, the pressure distribution behind the initiating shock in the liquid TNT is surely not the same in the experimental work and in the theoretical calculations. This may account for some of the difference. Since the calculated induction time is of the correct order of magnitude, and particularly since the t,X wave diagram for Case 2 is in qualitative agreement with experimental observations, it is felt that the model used in the above calculations is reasonable.

ACKNOWLEDGEMENTS

It is a pleasure to acknowledge the debt of the authors to a number of people for their help, advice, and encouragement during the progress of this work. Most of them are members of the Chemistry Research and Explosions Research Departments of the U.S. Naval Ordnance Laboratory. The authors are particularly grateful to Dr. Donna Price for critical review of the results, and to her and Dr. S. J. Jacobs for many helpful suggestions.

REFERENCES AND NOTES

1. F. B. Bowden and A. D. Yoffe, Initiation and Growth of Explosion in Liquids and Solids (Cambridge University Press, New York, 1952).
2. S. J. Jacobs, ARS J. 30, 151 (1960).
3. Marjorie W. Evans and C. M. Ablow, Chem. Revs. 61, 129 (1961).
4. A. Macek, Chem. Revs. 62, 41 (1962).
5. J. W. Enig and F. T. Metcalf, NOLTR 62-159 and NOLTR 62-160, in press.
6. H. W. Hubbard and M. H. Johnson, J. Appl. Phys. 30, 765 (1959).
7. J. von Neumann and R. D. Richtmyer, J. Appl. Phys. 21, 232 (1950).
8. J. W. Enig, Third Symposium on Detonation, Office of Naval Research Report ACR-52, Vol. 2 (1960), p. 534.
9. G. I. Taylor, Proc. Roy. Soc. (London) 200A, 235 (1950).
10. A. W. Campbell, W. C. Davis, and J. R. Travis, Phys. Fluids 4, 498 (1961).
11. The linear viscosity term is used here instead of the quadratic "q" term[7] (which is proportional to $(\partial u/\partial x)^2$) because the latter gives finite difference solutions which oscillate behind the shock front. This is undesirable in "marginal detonation" problems where a relatively few degrees make a difference in determining whether appreciable chemical reaction will occur. The coefficient μ in the linear viscosity term must be adjusted to give very smooth solutions and yet have the shock front spread over 5 or 6 mesh points. To do this, the coefficient μ must be delicately adjusted for different amplitude shocks in the same fluid, quite unlike the coefficient in the quadratic term.
12. W. B. Garn, J. Chem. Phys. 30, 819 (1959).

13. R. H. Cole, Underwater Explosions (Princeton University Press, New Jersey, 1948), p. 43.
14. It was first intended that Lucite be used as the gap material. However, comparison between the equation of state used in the computations and the equation of state for Lucite, when the latter became available [I. Jaffe, R. Beauregard, and A. Amster, ARS J. 32, 22 (1962)] showed that the former was inaccurate. It was not thought necessary to repeat, with the Lucite equation of state, the large number of computations since the results in the liquid TNT would show essentially the same behavior although arising from a different pressure distribution in the gap material. The effective compressibility of the gap material used is greater than that of Lucite.
15. J. W. Walsh and R. H. Christian, Phys. Rev. 97, 1544 (1955).
16. Donna Price, Chem. Revs. 59, 801 (1959).
17. W. R. Tomlinson, Jr. and O. E. Sheffield, Picatinny Arsenal Tech. Rept. 1740, Revision 1 (1958), p. 319.
18. A. J. B. Robertson, Trans. Faraday Soc. 44, 977 (1948).
19. Cited in Ref. 20.
20. W. B. Garn, J. Chem. Phys. 32, 653 (1960).
21. The hypervelocity wave phenomenon in the pre-compressed explosive, found also in the numerical calculations of Refs. 6 and 8, was used by R. F. Chaiken, M. S. thesis, Polytechnic Institute of Brooklyn, Brooklyn, New York (1958), to explain his experimental results on the shock initiation to detonation in nitromethane.
22. The value, $c_{v,\ell} = 0.328$ cal/(g deg), used in the computations is surely too low and, by Eq. (22), results in a temperature that is too high for given E and V. This leads to an initiating pressure P_t that is too

low. Use of higher, more realistic, values of c_v, would lead to increased values of P_t and hence better agreement with the experimental result. In Ref. 17, the values of c_v for solid TNT at 1 bar and 273, 293, 323, and 353°K are respectively, 0.309, 0.328, 0.353, and 0.374 cal/(g deg). In the liquid state at 354°K, c_v, is probably slightly less than 0.374 but it would increase with increasing P and T.

DISTRIBUTION LIST

	No. of Copies
SPIA (Distribution List)	99
Chief, Bureau of Naval Weapons Washington 25, D.C.	
Attn: Library (DLI-3)	1
Attn: SP-271	4
Attn: SP-20	1
Attn: SP-27	1
Attn: RMMP	3
Attn: F-12	1
Attn: RUME-32, E. M. Fisher	1
Attn: RUME-33, G. D. Edwards	1
Office of Naval Research, Washington 25, D.C. Attn: Power Branch (Code 429)	2
Aerojet-General Corporation 1711 Woodruff Avenue, Downey, California Attn: Dr. L. Zernow	3
Aerojet-General Corporation P.O. Box 1168, Sacramento, California Attn: Dr. W. Kirchner	4
Lockheed Missiles and Space Company A Division of Lockheed Aircraft Corporation 1122 Jagels Road, Sunnyvale, California Attn: Mr. J. Lightfoot	3
Bureau of Naval Weapons Representative (Special Projects Office) Lockheed Missiles and Space Company P.O. Box 504, Sunnyvale, California Attn: SPL-313	2
Bureau of Naval Weapons Resident Representative (Special Projects Office) Aerojet-General Corporation Sacramento, California Attn: SPLA-30	2
Bureau of Naval Weapons Branch Representative Allegany Ballistics Laboratory Cumberland, Maryland Attn: SPH-30	2
Allegany Ballistics Laboratory Hercules Power Company Cumberland, Maryland Attn: Dr. N. F. LeBlanc Mr. R. Richardson	4

DISTRIBUTION LIST (Cont'd.)

	No. of Copies
Aeronutronics A Division of Ford Motor Company Ford Road, Newport Beach, California Attn: Mr. S. Weller Mr. M. Boyer	3
Rohm and Haas Company Redstone Arsenal Huntsville, Alabama Attn: Dr. H. Shuey	3
Commander, U.S. Naval Ordnance Test Station China Lake, California Attn: Code 453	2
Attn: Code 5008	1
Armed Services Explosives Safety Board Building T-7, Gravelly Point Washington, D.C. Attn: Mr. R. C. Herman	1
Stanford Research Institute Liquid Propellant Department Propulsion Sciences Division Menlo Park, California Attn: Dr. A. B. Amster	3
U.S. Bureau of Mines 4800 Forbes Street, Pittsburgh 13, Pennsylvania Attn: Dr. C. M. Mason	1
Director, Office of the Secretary of Defense Adv. Res. Proj. Agency, Washington 25, D.C. Attn: Dr. John F. Kincaid	1
University of Cal. Lawrence Radiation Lab. P.O. Box 808, Livermore, California Attn: Dr. G. Dorough	1
Los Alamos Scientific Laboratory P.O. Box 1663, Los Alamos, New Mexico Attn: Dr. L. C. Smith	1
Liquid Propellant Information Agency The Johns Hopkins University Applied Physics Laboratory 8621 Georgia Avenue, Silver Spring, Maryland	25
Space Technology Laboratory P.O. Box 95001, Los Angeles 45, California Attn: Mr. H. A. Taylor VIA	1
Navy Liaison Office (SP) Air Force Unit Post Office Los Angeles 45, California Attn: M. H. Holt	1

CATALOGING INFORMATION FOR LIBRARY USE

BIBLIOGRAPHIC NFORMATION

	DESCRIPTORS	CODES		DESCRIPTORS	CODES
SOURCE	NOL technical report	NOLTR	SECURITY CLASSIFICATION AND CODE COUNT	Unclassified - 34	UØ34
REPORT NUMBER	62-159	62Ø159	CIRCULATION LIMITATION		
REPORT DATE	24 August 1962	Ø862	CIRCULATION LIMITATION OR BIBLIOGRAPHIC		
			BIBLIOGRAPHIC (SUPPL., VOL., ETC.)		

SUBJECT ANALYSIS OF REPORT

DESCRIPTORS	CODES	DESCRIPTORS	CODES	DESCRIPTORS	CODES
Shock	SHOC	Reaction	REAT	Time	TIME
Initiation	INTI	Explosive	EXPL	Pressure	PRES
Liquid	LIQU	Cells	CELL	One-dimensional	ONED
TNT	TNTE	Velocity	VELC	Gap tests	GAPT
Theoretical	THEY	Numerical	NUMB	Interface	INTF
Calculations	COMA	Experiments	EXPE	Front	FRON
Homogeneous	HOMO	Partial	PARI	Temperature	TEMP
Growth	GROW	Differential	DIFE	Equations-of-state	EQUS
Detonation	DETO	Equations	EQUA	Finite	FNIT
Explosion	EXPS	Hydrodynamics	HYDN	Comparison	CMRI
Waves	WAVE	Sensitivity	SENV		
Chemical	CHEM	Induction	INDU		

Naval Ordnance Laboratory, White Oak, Md.
(NOL technical report 62-159)
THEORETICAL CALCULATIONS ON THE SHOCK INITIATION OF LIQUID TNT, by Julius W. Enig and Fred T. Metcalf. 24 Aug. 1962. 30p. tables, diagr. NOL task FR-59 UNCLASSIFIED

Theoretical calculations describing initiation phenomena in homogeneous liquid TNT, produced by shocks between 80 and 89 kilobars, are given. Initiation mechanism and growth to detonation are shown to be in semi-quantitative agreement with experimental results. Numerical experiments, which are based on finite difference solutions of partial differential equations of hydrodynamics, show extreme sensitivity of induction time to initiating pressure in idealized one-dimensional gap tests.

1. Explosives - Initiation
2. Explosives - Shock waves
3. Explosives - Pressure
4. TNT - Detonation

I. Title
II. Enig, Julius W.
III. Metcalf, Fred T., jt. author
IV. Project

Naval Ordnance Laboratory, White Oak, Md.
(NOL technical report 62-159)
THEORETICAL CALCULATIONS ON THE SHOCK INITIATION OF LIQUID TNT, by Julius W. Enig and Fred T. Metcalf. 24 Aug. 1962. 30p. tables, diagr. NOL task FR-59 UNCLASSIFIED

Theoretical calculations describing initiation phenomena in homogeneous liquid TNT, produced by shocks between 80 and 89 kilobars, are given. Initiation mechanism and growth to detonation are shown to be in semi-quantitative agreement with experimental results. Numerical experiments, which are based on finite difference solutions of partial differential equations of hydrodynamics, show extreme sensitivity of induction time to initiating pressure in idealized one-dimensional gap tests.

1. Explosives - Initiation
2. Explosives - Shock waves
3. Explosives - Pressure
4. TNT - Detonation

I. Title
II. Enig, Julius W.
III. Metcalf, Fred T., jt. author
IV. Project

Naval Ordnance Laboratory, White Oak, Md.
(NOL technical report 62-159)
THEORETICAL CALCULATIONS ON THE SHOCK INITIATION OF LIQUID TNT, by Julius W. Enig and Fred T. Metcalf. 24 Aug. 1962. 30p. tables, diagr. NOL task FR-59 UNCLASSIFIED

Theoretical calculations describing initiation phenomena in homogeneous liquid TNT, produced by shocks between 80 and 89 kilobars, are given. Initiation mechanism and growth to detonation are shown to be in semi-quantitative agreement with experimental results. Numerical experiments, which are based on finite difference solutions of partial differential equations of hydrodynamics, show extreme sensitivity of induction time to initiating pressure in idealized one-dimensional gap tests.

1. Explosives - Initiation
2. Explosives - Shock waves
3. Explosives - Pressure
4. TNT - Detonation

I. Title
II. Enig, Julius W.
III. Metcalf, Fred T., jt. author
IV. Project

Naval Ordnance Laboratory, White Oak, Md.
(NOL technical report 62-159)
THEORETICAL CALCULATIONS ON THE SHOCK INITIATION OF LIQUID TNT, by Julius W. Enig and Fred T. Metcalf. 24 Aug. 1962. 30p. tables, diagr. NOL task FR-59 UNCLASSIFIED

Theoretical calculations describing initiation phenomena in homogeneous liquid TNT, produced by shocks between 80 and 89 kilobars, are given. Initiation mechanism and growth to detonation are shown to be in semi-quantitative agreement with experimental results. Numerical experiments, which are based on finite difference solutions of partial differential equations of hydrodynamics, show extreme sensitivity of induction time to initiating pressure in idealized one-dimensional gap tests.

1. Explosives - Initiation
2. Explosives - Shock waves
3. Explosives - Pressure
4. TNT - Detonation

I. Title
II. Enig, Julius W.
III. Metcalf, Fred T., jt. author
IV. Project